

Reaction Theory

Stefan Typel

GSI Helmholtzzentrum für Schwerionenforschung GmbH, Planckstraße 1, 64291 Darmstadt, Germany

Received: date / Revised version: date

Abstract. Reactions with atomic nuclei play a pivotal role in the experimental study of nuclei. They are a tool in order to obtain crucial information on nuclear structure of nuclei, in particular for unstable nuclei far off the valley of stability. Besides the investigation of nuclear properties, nuclear reactions can be used as indirect methods to extract cross sections of astrophysical interest that cannot be measured directly in the laboratory. After an overview over the variety of nuclear reactions and their major characteristics, the basic formalism of reaction theory is introduced and essential concepts are presented in order to describe direct reactions. The main challenges in the future development of reaction theory are addressed.

PACS. 24.10.-i Nuclear reaction models and methods – 24.50.+g Direct reactions – 24.87.+y Surrogate reactions

1 Introduction

The detailed study of nuclear properties relies mostly on reaction experiments in the laboratory. The interpretation of their results requires a comparison with theoretical calculations utilizing reaction theory that is appropriate for the considered processes. Besides the investigation of nuclear structure, nuclear reactions itself are of interest, e.g. in astrophysical applications. Many approaches in reaction theory have been developed over the last decades. They were successfully applied in the analysis of experimental data and deep insights into the mechanisms of a large variety of reactions were attained.

The interest in reaction theory has been revived in recent years due to the investigation of unstable, neutron or proton rich nuclei far off the valley of stability. The advent of radioactive beam facilities made it possible to study these short-lived nuclei, which were not accessible before. The unique peculiarities of exotic nuclei demand to reassess the validity of widely used theoretical approaches and to develop new methods that are suitable for the conditions of the employed reactions.

This contribution serves as an introduction to the basic methods and concepts in reaction theory so that a comprehension of current developments and applications becomes possible. Here it should suffice to give the essence of the theoretical description. An in-depth delineation of the formalism with a full derivation of the relevant formulas can be found in many excellent textbooks on reaction theory, see, e.g., references [1–15]. In this work, completeness can not be achieved and many topics have to be left out. This paper is not a review of recent results or specific theoretical approaches for individual cases. For that purpose, the interested reader is invited to explore the relevant literature himself/herself. Since there is such a multitude of

reactions and similarly a large number of theoretical approaches, only a selection of topics, mainly connected to direct reactions, will be covered. Other types of reactions, e.g. compound nucleus reactions or heavy-ion collisions, are not dealt with here. Some additional restrictions apply in this presentation. Nonrelativistic kinematics will be supposed and antisymmetrization is not considered explicitly. Weak interaction processes are not treated and the spins of particles are neglected in most cases with a few exceptions.

There are two major parts in this work. General aspects of reaction theory are presented in the first section with an overview over the main theoretical approaches. More details are considered in the second section, which contains a selection of applications. It is followed by a short summary.

2 Fundamentals of reaction theory

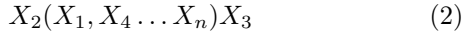
All processes that occur if two or more particles collide within an interaction zone can be considered as reactions. The extent of this zone in coordinate space depends on the range of the interaction and thus can be very different. If the reaction mechanism is ruled by the long-range electromagnetic forces, particles can interact over much larger distances than in processes with the short-range strong or weak interactions. In many instances different types of interactions compete in a reaction and interference effects can occur.

Distinct notations for reactions have been established in the past. In laboratory experiments, in most of the cases it is only possible to study reactions with two particles (X_1, X_2) in the initial state. With $n - 2$ particles ($X_3,$

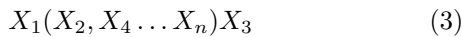
\dots, X_n) in the final state, the form



can be used as in chemistry. If one wants to distinguish the projectile X_1 , the target X_2 and the (detected) ejectiles X_4, \dots, X_n , the alternative notation



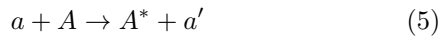
is often employed. If X_2 is an instable nucleus it is usually not possible to produce a target from this material. Then inverse kinematics are used, i.e. X_1 and X_2 are interchanged leading to



with projectile X_2 and target X_1 . Even with the limitation to reactions with only two colliding particles, there is large variety of reaction types. The most simple process is the elastic scattering



without a change of the particles identities. In an inelastic scattering



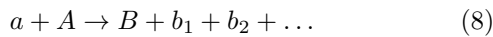
one particle can be excited (denoted by the asterisk) and the other one loses a part of its energy (indicated by the prime). Rearrangement reactions



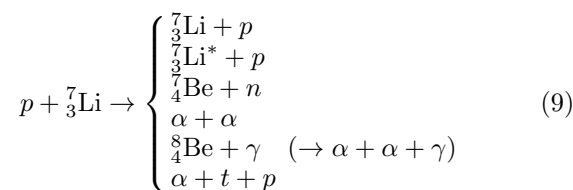
with $b \neq a$ and $B \neq A$ are usually realized by the exchange of nucleons in a transfer reaction. A particular case is a radiative capture reaction



where two nuclei fuse to form a compound nucleus C with the emission of a photon. Instead of two particles in the final state as above, there is a large number of possible final states in many-body reactions



with more than two ejectiles. As an example, the collision of a proton with a ${}^7\text{Li}$ nucleus



produces a number of different final states.

2.1 Length, time and energy scales

Every reaction can be characterized by specific length and time scales. It is useful to consider the radius R of a nucleus (assumed to be spherical), the corresponding area of a circle $S = \pi R^2$, and the time $t = 2R/c$ for light to transverse the nucleus. The radius of a stable nucleus of mass number A can be estimated to be $R \approx r_0 A^{1/3}$ with $r_0 = 1.25 \text{ fm} = 1.25 \cdot 10^{-13} \text{ cm}$. For a ${}^{208}\text{Pb}$ nucleus the values $R \approx 7.4 \text{ fm}$, $S \approx 172 \text{ fm}^2 = 1.72 \text{ b}$ and $t \approx 14.8 \text{ fm}/c \approx 4.9 \cdot 10^{-23} \text{ s}$ are found. Here, the unit *barn* for areas in nuclear reaction theory with $1 \text{ b} = 10^{-28} \text{ m}^2$ or $1 \text{ fm}^2 = 10 \text{ mb}$ has been introduced. The time scales for reactions can vary substantially. Fast reactions proceed within a period of approx. 10^{-22} s . These are typically direct reactions where few nucleons are involved in single-step processes. Multistep reactions take somewhat longer and more complicated reaction mechanisms are involved. In slow reactions with a duration much longer than 10^{-22} s a compound nucleus is formed and many nucleons take part in the process, often inducing collective excitations. In most cases the memory of the initial state is lost and the reaction is dominated by statistical features. Evidently, the theoretical description of fast and slow reactions will be less involved than that of intermediate reactions.

Nuclear reactions can also be distinguished according to the typical collision energies. A very large range is actually covered in experiments from reactions with thermal neutrons of approx. 25 meV, via astrophysical reactions with a few 10 or 100 keV, direct nucleon transfer reactions with a few MeV per nucleon, to Coulomb excitation reactions with a few 10 or 100 MeV per nucleon or even relativistic heavy-ion collisions with a few GeV or TeV per nucleon. This can be compared to the typical energy scales for nuclear binding and excitation energies in the order of a few MeV or that of the involved potentials, e.g., the height of the Coulomb barrier $E_C = Z_a Z_A e^2 / R_C$ with the charge numbers Z_a, Z_A of the colliding nuclei and the square of the electric charge unit $e^2 \approx 1.44 \text{ MeV fm}$. The distance R_C can be estimated as the sum $R_a + R_A$ of the nuclear radii. Clearly, the magnitude of the collision energy will have a major impact on the reaction mechanism and the choice of the theoretical description.

Another important quantity is the Q value, defined by

$$Q = (m_a + m_A - m_b - m_B) c^2 \quad (10)$$

for a reaction $A(a, b)B$. It is determined by the masses m_i ($i = A, a, b, B$) of the participating nuclei. A generalization to other types of reactions is obvious. Reactions with positive Q value are exothermic, i.e. there is an release of kinetic energy due to a larger binding of the nuclei in the final state than in the initial state. Elastic reactions are characterized by $Q = 0$ and for negative Q values the reaction is endothermic. In this case there is a energy threshold in the initial state below which the reaction cannot proceed.

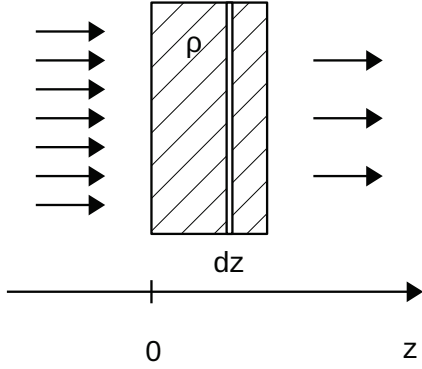


Fig. 1. Attenuation of a uniform beam of particles hitting a thick target of density ρ due to reactions.

2.2 Conservation laws

Not every reaction that can be imagined can actually occur in reality. There is a limitation due to the existence of several conservation laws, which are consequences of symmetries that apply to nuclear reactions. The most prominent is probably the law of energy conservation. If we consider again a reaction $A(a, b)B$, it can be expressed as follows. The total energy in the initial state

$$E(a + A) = T_a + T_A + (m_a + m_A)c^2, \quad (11)$$

containing kinetic energies T_i and masses m_i of the nuclei, has to be identical to that in the final state

$$E(b + B) = T_b + T_B + (m_b + m_B)c^2. \quad (12)$$

Similarly, there is a conservation of the total momentum

$$\mathbf{P}(a + A) = \mathbf{p}_a + \mathbf{p}_A = \mathbf{p}_b + \mathbf{p}_B = \mathbf{P}(b + B) \quad (13)$$

and of the total angular momentum

$$\begin{aligned} \mathbf{J}(a + A) &= \mathbf{J}_a + \mathbf{J}_A \\ &= \mathbf{J}_b + \mathbf{J}_B = \mathbf{J}(b + B) \end{aligned} \quad (14)$$

where J_i contains the intrinsic angular momentum or spin of a particle i as well as the orbital angular momentum with respect to a given reference point in space, usually chosen as the center of mass. Besides these kinematic quantities, the particles carry some additional quantum numbers that give rise to additional conservation laws. Examples are the parity

$$\begin{aligned} P(a + A) &= P_a \cdot P_A \cdot (-1)^{l_{aA}} \\ &= P_b \cdots P_B \cdot (-1)^{l_{bB}} = P(b + B), \end{aligned} \quad (15)$$

with orbital angular momenta of relative motion l_{aA} and l_{bB} , which is a multiplicative quantum number because of a discrete symmetry, and the total isospin

$$\mathbf{T}(a + A) = \mathbf{T}_a + \mathbf{T}_A = \mathbf{T}_b + \mathbf{T}_B = \mathbf{T}(b + B) \quad (16)$$

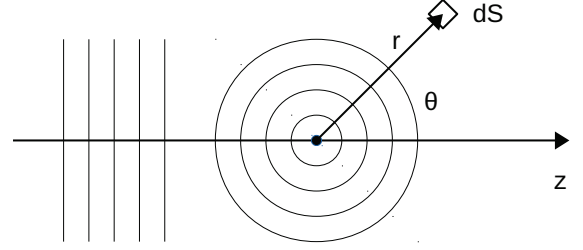


Fig. 2. Scattering of a beam of particles on a single target with detection at a distance r under a scattering angle θ .

that is analogous to the total angular momentum but in an abstract isospin space. In addition, there is a conservation of charge, baryon and lepton numbers. However, depending on the type of interaction that mediates the reaction, not all conservation laws apply to all reactions. E.g., in electromagnetically induced reactions, there is no conservation of the total isospin \mathbf{T} but only the projection T_z on a single axis in isospin space.

2.3 Definition of cross sections

Independent of the theoretical description of a reaction, may it be with classical, semiclassical or quantal methods, observables have to be defined that can be measured in experiments and compared to theory. The essential quantities are cross sections that measure the strength of a reaction. In the most simple case, the following situation can be imagined. A uniform beam of particles moving in positive z -direction, see figure 1, hits a thick target of constant number density ρ at $z = 0$. The occurrence of reactions reduces the intensity of the beam depending on the penetration depth z inside the target. The reduction of the current J over an infinitesimally small length dz is proportional to the current itself and the target density ρ . This can be formulated mathematically as a simple first order differential equation

$$\frac{dJ}{dz} = -\sigma J(z)\rho \quad (17)$$

with a proportionality constant σ , the (interaction) cross section. The solution of equation (17) is simply given by the law of exponential decrease

$$J(z) = J(0) \exp(-\sigma\rho z). \quad (18)$$

Denoting with L and T the dimensions of length and time, respectively, one has the dimensions of the current $[J] = L^{-2}T^{-1}$ and number density $[\rho] = L^{-3}$. Hence, the unit of the cross section $[\sigma] = L^2$ is an area, usually measured in barns in nuclear physics, see section 2.1. The cross section depends on the energy E of the incident beam and $\sigma(E)$ is called the excitation function.

More detailed information on the reaction process is obtained when the final products are detected and the

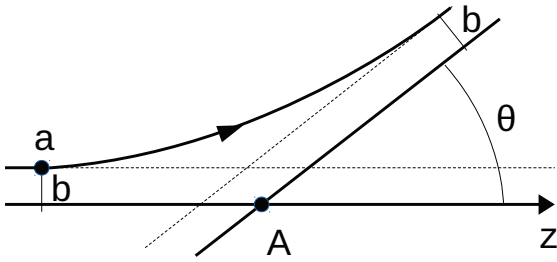


Fig. 3. Classical trajectory of a particle a with impact parameter b scattered at a target A under a scattering angle θ .

dependence on the scattering angle θ is considered leading to the definition of a differential cross section $d\sigma/d\Omega$. The initial state is again given by a uniform beam of particles moving in z direction with current J_i that interacts with a single target at a fixed position. Ejectiles are observed in a detector with area dS at a distance r from the target, see figure 2. With the current J_f in the final state at the detector in radial direction, the cross section is defined as

$$d\sigma_{fi} = \frac{J_f dS}{J_i}. \quad (19)$$

Introducing the solid angle $d\Omega$ via

$$dS = r^2 d\Omega \quad (20)$$

the differential scattering cross section is found as

$$\frac{d\sigma_{fi}}{d\Omega} = \frac{J_f r^2}{J_i} \quad (21)$$

with the currents J_i and J_f that can be calculated, e.g., in a quantal description of the scattering process, see section 2.4.

2.3.1 Classical description

In classical physics, the differential cross section for elastic scattering is given by

$$\frac{d\sigma}{d\Omega} = \frac{b}{\sin\theta} \left| \frac{d\theta}{db} \right|^{-1} \quad (22)$$

with the deflection function $\theta(b)$ depending on the impact parameter b when azimuthal symmetry, i.e. independence on the angle ϕ , is presumed. The relation between θ and b , see figure 3, is obtained by determining the classical trajectories of the scattered particle. They are found by solving the Newtonian equations of motion

$$m_i \ddot{\mathbf{r}}_i = \mathbf{F}_i \quad (23)$$

with the position depending force \mathbf{F}_i for given initial conditions, i.e. position and velocity or momentum of the particle i . Thus a set of coupled ordinary time-dependent differential equations has to be solved. Alternatively conservation laws for energy, momentum and angular momentum can be used. A simple example is the elastic scattering

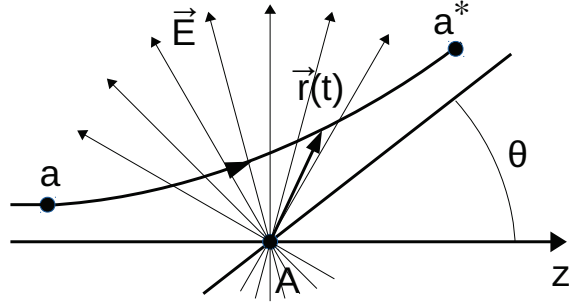


Fig. 4. Coulomb excitation of a projectile a in the electric field \mathbf{E} of a target A during the scattering with angle θ .

of a particle a with energy E and impact parameter b on a target A . With the Coulomb force

$$\mathbf{F}_a = \frac{Z_a Z_A e^2}{r^2} \frac{\mathbf{r}}{r} \quad (24)$$

acting on a the deflection function

$$\theta(b) = 2 \operatorname{arccot} \left(\frac{2bE}{Z_a Z_A e^2} \right) \quad (25)$$

is deduced. With relation (22) the classical Rutherford cross section for elastic scattering

$$\frac{d\sigma_R}{d\Omega} = \left(\frac{Z_a Z_A e^2}{4E} \right)^2 \frac{1}{\sin^4(\frac{\theta}{2})} \quad (26)$$

is obtained.

2.3.2 Semiclassical description

In the classical approach, only the elastic scattering of a particle under the action of a potential or force can be treated. The excitation of the scattered particle a , however, requires to include a quantal description. A prominent example of this approach is the Coulomb excitation of a nucleus during the quasi-elastic scattering on a charged target. In this case, the projectile a at position $\mathbf{r}(t)$ experiences a time-dependent potential

$$V(t) = \sum_{i \in a} \frac{Z_i Z_A e^2}{|\mathbf{r}(t) + \mathbf{x}_i|} - \frac{Z_a Z_A e^2}{|\mathbf{r}(t)|} \quad (27)$$

that depends on the positions \mathbf{x}_i of nucleons i inside a . The differential excitation cross section can be factorized as

$$\frac{d\sigma_{fi}}{d\Omega} = \frac{d\sigma_R}{d\Omega} \times P_{fi} \quad (28)$$

with the elastic Rutherford cross section and an excitation probability P_{fi} that describes the likelihood of the excitation of a from the initial ground state $|i\rangle$ to a final state $|f\rangle$. This quantity is determined as

$$P_{fi} = |a_{fi}|^2 \quad (29)$$

with the excitation amplitude

$$a_{fi} = \frac{1}{i\hbar} \int_{-\infty}^{\infty} dt e^{-i\omega t} \langle f | V(t) | i \rangle \quad (30)$$

in first-order time-dependent perturbation theory with excitation energy $\hbar\omega$. The Coulomb excitation method has been widely applied to study the properties of excited states of stable nuclei [16,17]. It also has become a valuable tool to investigate electromagnetically induced reactions and the structure of nuclei with a low threshold for the excitation to unbound states in the continuum [18, 19]. In this case, the projectile a breaks up into pieces that can be detected individually. This Coulomb dissociation method is applied favorably to the study of exotic nuclei.

The combination of classical and quantal methods in the semiclassical approach, however, is not valid in all cases. A condition for the validity is that the Sommerfeld parameter η of the $a + A$ scattering, see section 3.1.1 for the definition, is sufficiently larger than one. Otherwise a fully quantal approach has to be used.

2.3.3 Quantal description

The most general description of reactions is based on a fully quantal treatment. This requires to determine the complete wave function ψ of the system by solving the many-body Schrödinger equation for the specific boundary conditions of scattering. There are two possible paths that are explored in actual calculations. The first method tries to solve the time-dependent Schrödinger equation

$$i\hbar \frac{\partial}{\partial t} \psi = \hat{H} \psi \quad (31)$$

with Hamiltonian \hat{H} . This is usually done by following the time evolution of a wave packet that describes the projectile interacting with the target. Despite its merits, this approach is not considered in the following.

In the second method, the stationary Schrödinger equation

$$\hat{H} \psi = E \psi \quad (32)$$

for a fixed energy E is solved for the appropriate boundary conditions. They can be formulated as 'plane-wave + outgoing (ingoing) spherical waves'. This will be elaborated in more detail below. There are two possible formulations. The first one directly tries to use the stationary Schrödinger equation (32) as a partial differential equation. But it is also possible to reformulate the problem as an integral equation. Both approaches will be presented in section 2.4.

In the quantal description of reactions it is convenient to define channels c that characterize the asymptotic states of the system when the particles are well separated and their mutual interaction becomes sufficiently small. These channels are characterized by a partition, e.g., $A+a$, $B+b$, or $C + \gamma$ and by specifying additional quantum number that are needed to identify the state completely. This includes, e.g., the energies and momenta of the particles.

2.4 Stationary scattering theory

The theoretical formulation for reactions with nuclei a and A in the initial channel starts with the definition of the total Hamiltonian. It reads

$$\hat{H} = \hat{H}_a + \hat{H}_A + \hat{T}_{aA} + \hat{V}_{aA} \quad (33)$$

with the Hamiltonians \hat{H}_a and \hat{H}_A in the Schrödinger equations

$$\hat{H}_a \phi_a = E_a \phi_a \quad (34)$$

and

$$\hat{H}_A \phi_A = E_A \phi_A \quad (35)$$

for the colliding particles with total energies (including rest masses) E_a and E_A , respectively. Thus, the wave functions ϕ_a and ϕ_A describe the internal structure of the nuclei. The kinetic energy operator of relative motion

$$\hat{T}_{aA} = -\frac{\hbar^2}{2\mu_{aA}} \Delta_{\mathbf{r}_{aA}} \quad (36)$$

in equation (33) acts on the relative coordinate

$$\mathbf{r}_{aA} = \mathbf{r}_a - \mathbf{r}_A \quad (37)$$

and contains the reduced mass

$$\mu_{aA} = \frac{m_a m_A}{m_a + m_A}. \quad (38)$$

\hat{V}_{aA} denotes the interaction potential between a and A . In general, it depends on the coordinates of all nucleons inside the interacting nuclei and not only on \mathbf{r}_{aA} . For the Hamiltonian

$$\hat{H}_0^{(i)} = \hat{H}_a + \hat{H}_A + \hat{T}_{aA} = \hat{H} - \hat{V}_{aA} \quad (39)$$

in the initial state without the interaction potential \hat{V}_{aA} the solutions of the Schrödinger equation

$$\hat{H}_0^{(i)} \Phi_i = (E_a + E_A + E_{aA}) \Phi_i \quad (40)$$

are easily found as plane waves

$$\Phi_i = \phi_i \exp(i\mathbf{k}_i \cdot \mathbf{r}_i) \quad (41)$$

with

$$\phi_i = \phi_a \phi_A, \quad (42)$$

$\mathbf{r}_i = \mathbf{r}_{aA}$, and the relative momentum

$$\mathbf{k}_i = \mathbf{k}_{aA} = \mu_{aA} \left(\frac{\mathbf{k}_a}{m_a} - \frac{\mathbf{k}_A}{m_A} \right), \quad (43)$$

which enters in the energy

$$E_{aA} = \frac{\hbar^2 k_i^2}{2\mu_{aA}} \quad (44)$$

of relative motion. The above quantities can be introduced in a similar manner for all possible final channels of a reaction.

The full solutions of the Schrödinger equation

$$\hat{H}\Psi_i^{(\pm)} = E\Psi_i^{(\pm)} \quad (45)$$

with initial channel i are denoted by $\Psi_i^{(\pm)}$ where the '+' ('-') solution corresponds to a wave function with asymptotically outgoing (ingoing) spherical waves in all final channels. The meaning of these boundary conditions becomes more apparent when the asymptotic form of $\Psi_i^{(\pm)}$ for large radii is written as

$$\Psi_i^{(\pm)} \rightarrow \Phi_i + \sum_f \phi_f f_{fi}^{(\pm)} \frac{\exp(\pm ik_f r_f)}{r_f} \quad (46)$$

with scattering amplitudes $f_{fi}^{(\pm)}$ for all final channels f . The wave function Φ_i is the plane-wave solution (41) of equation (40) and ϕ_f is the product of the individual particle wave functions in the final state, e.g., $\phi_f = \phi_b \phi_B$ for the channel $f = b + B$.

The differential cross section for the reaction from an initial channel i to a final channel f can be calculated according to equation (21) if the currents J_i and J_f of relative motion are known. In nonrelativistic quantum mechanics the current of a particle m with wave function ψ is given by

$$\mathbf{J} = \frac{\hbar}{2mi} [\psi^* (\nabla \psi) - (\nabla \psi^*) \psi] . \quad (47)$$

This relation can be applied to the current case. The mass m is replaced by the reduced mass and ψ by the appropriate wave function. In the initial state, the wave function of relative motion

$$\psi = \exp(i\mathbf{k}_i \cdot \mathbf{r}_i) \quad (48)$$

leads to the current

$$\mathbf{J}_i = \frac{\hbar \mathbf{k}_i}{\mu_i} = \mathbf{v}_i = \mathbf{v}_{aA} , \quad (49)$$

which is simply the velocity of relative motion. For an outgoing spherical wave

$$\psi = f_{fi}^{(+)} \frac{\exp(ik_f r_f)}{r_f} \quad (50)$$

the leading term of the asymptotic form of the current

$$\mathbf{J}_f \rightarrow \frac{|f_{fi}^{(+)}|^2}{r_f^2} \frac{\hbar \mathbf{k}_f}{\mu_f} \frac{\mathbf{r}_f}{r_f} = \frac{|f_{fi}^{(+)}|^2}{r_f^2} \mathbf{v}_f \quad (51)$$

contains the modulus square of the scattering amplitude and decreases proportional to the inverse square of the relative distance r_f . Combining these result, the differential reaction cross section can be expressed as

$$\frac{d\sigma_{fi}}{d\Omega} = \frac{J_f r_f^2}{J_i} = \frac{v_f}{v_i} |f_{fi}^{(+)}|^2 . \quad (52)$$

Thus the knowledge of the scattering amplitude $f_{fi}^{(+)}$, i.e., the asymptotic form of the total wave function $\Psi_i^{(+)}$ is sufficient for the calculation of $d\sigma_{fi}/d\Omega$. In contrast to the discussion in section 2.3, the dimension of the currents (49) and (51) is LT^{-1} since the wave functions are not normalized to the number of particles per volume. However, the result for the differential cross section is unaffected by this difference.

There are different avenues to determine scattering amplitudes in theoretical descriptions of reactions. Two major approaches are delineated in the following two sections.

2.4.1 Partial wave expansion

A widely used method to represent the full scattering wave function is based on an expansion in partial waves. Considering an elastic scattering reaction $A(a, a)A$ in a simple spherical short-range potential $V_{aA}(r)$, the single-channel form¹

$$\Psi_i^{(+)} = \sum_{l=0}^{\infty} \sum_{m=-l}^l \frac{\varphi_l^{(+)}(r)}{r} Y_{lm}(\hat{r}) \phi_i \quad (53)$$

with a summation over orbital angular momenta l and their projection m is the appropriate ansatz. For a generalisation with arbitrary spins of the particles see, e.g., reference [20]. The wave functions of radial motion are denoted by $\varphi_l^{(+)}$ and Y_{lm} are spherical harmonics depending on the direction $\hat{r} = \mathbf{r}/r$. The factor ϕ_i is again the product of the internal wave functions of the scattered particles. A separation of variables in equation (45) leads to the radial Schrödinger equation

$$E_{aA} \varphi_l^{(+)}(r) = \left[-\frac{\hbar^2}{2\mu_{aA}} \frac{d^2}{dr^2} + \frac{l(l+1)}{r^2} + \hat{V}_{aA}(r) \right] \varphi_l^{(+)}(r) \quad (54)$$

to determine the functions $\varphi_l^{(+)}$. Solutions of this second-order differential equation have to be found with the correct boundary conditions. Continuity of the total wave function at the origin requires $\varphi_l^{(+)}(r) = 0$ for $r = 0$. For $r \rightarrow \infty$ the radial wave functions have to be solutions of equation (54) with vanishing potential \hat{V}_{aA} . Hence they must be linear combinations of regular and irregular spherical Bessel functions [21]. This is only correct for short-range potentials. Modifications apply, e.g., for a long-range Coulomb potential, see section 3.1.1 for details. As noticed before, solutions of the full Schrödinger equation (45) with $\hat{V}_{aA} = 0$ are given by equation (41) with the expansion

$$\Phi_i = 4\pi \sum_{l,m} i^l j_l(k_i r) Y_{lm}(\hat{r}) Y_{lm}^*(\hat{k}_i) \phi_i \quad (55)$$

¹ The index i of \mathbf{r}_i is suppressed in the following.

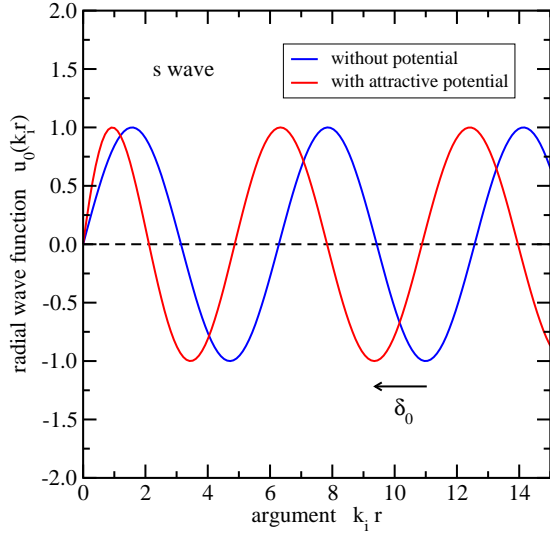


Fig. 5. Radial wave function in partial wave $l = 0$ without the action of potential (blue line) and with potential (red line).

with $\hat{k}_i = \mathbf{k}_i/k_i$ and regular spherical Bessel functions j_l . For $l = 0$ one has

$$j_0(z) = \frac{\sin z}{z} = \frac{e^{iz} - e^{-iz}}{2iz}. \quad (56)$$

For angular momenta $l > 0$ the spherical Bessel functions can be determined as derivatives

$$j_l(z) = z^l \left(-\frac{1}{z} \frac{d}{dz} \right)^l j_0(z). \quad (57)$$

Similar as for j_0 , they can be written as a difference

$$j_l(z) = \frac{1}{2iz} \left[u_l^{(+)}(z) - u_l^{(-)}(z) \right] \quad (58)$$

with functions $u_l^{(\pm)}$ which have the asymptotic behavior

$$u_l^{(\pm)}(z) \rightarrow \exp \left[\pm i \left(z - l \frac{\pi}{2} \right) \right] \quad (59)$$

for arguments $z \rightarrow \infty$. Using this representation, the expansion of the plane-wave solution becomes

$$\begin{aligned} \Phi_i &= \frac{4\pi}{2ik_i r} \sum_{l,m} i^l \left[u_l^{(+)}(k_i r) - u_l^{(-)}(k_i r) \right] \\ &\times Y_{lm}(\hat{r}) Y_{lm}^*(\hat{k}_i) \phi_i. \end{aligned} \quad (60)$$

The action of the scattering potential \hat{V}_{aA} modifies the form of the radial wave functions $\varphi_l^{(+)}(r)$. For large distances, however, they still have to be a linear combination of spherical Bessel functions or the functions $u_l^{(\pm)}$. Since $u_l^{(-)}$ corresponds to an ingoing spherical wave that cannot be affected by the scattering process, only the outgoing spherical wave can be modified. Hence a complex factor S_l , which generally depends on the momentum k_i ,

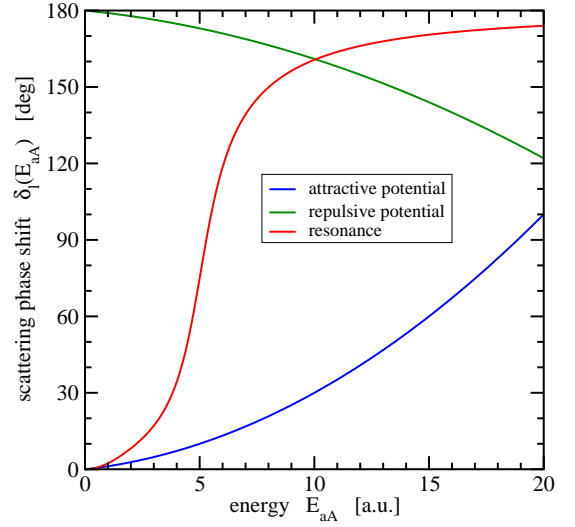


Fig. 6. Dependence of the scattering phase shift δ_l in partial wave l on the energy E_{aA} in the initial state for an elastic scattering process $A(a, a)A$.

is introduced in front of $u_l^{(+)}$ in the asymptotic form

$$\begin{aligned} \Psi_i^{(+)} &\rightarrow \frac{4\pi}{2ik_i r} \sum_{l,m} i^l \left[S_l(k_i) u_l^{(+)}(k_i r) - u_l^{(-)}(k_i r) \right] \\ &\times Y_{lm}(\hat{r}) Y_{lm}^*(\hat{k}_i) \phi_i \end{aligned} \quad (61)$$

of the solution of the full Schrödinger equation (45). The difference between the full solution $\Psi_i^{(+)}$ and the plane wave Φ_i corresponds to the scattered part

$$\begin{aligned} \Psi_i^{(+)} - \Phi_i &\rightarrow \frac{4\pi}{2ik_i r} \sum_{l,m} i^l [S_l(k_i) - 1] u_l^{(+)}(k_i r) \\ &\times Y_{lm}(\hat{r}) Y_{lm}^*(\hat{k}_i) \phi_i \end{aligned} \quad (62)$$

of the wave function. Comparing with equation (46) for $f = i$ yields the expression

$$f_{ii}^{(+)}(\theta) = \sum_l \frac{2l+1}{2ik_i} [S_l(k_i) - 1] P_l(\cos \theta) \quad (63)$$

for the elastic scattering amplitude with Legendre polynomials P_l , which depend on the cosine of the scattering angle $\cos \theta = \hat{r} \cdot \hat{k}_i$. They were introduced with help of the relation

$$(2l+1)P_l(\cos \theta) = 4\pi \sum_m Y_{lm}(\hat{r}) Y_{lm}^*(\hat{k}_i). \quad (64)$$

One sees that the scattering amplitude is determined by the so-called S matrix elements S_l that can be conveniently written as

$$S_l = \exp(2i\delta_l) \quad (65)$$

with scattering phase shifts δ_l .

In the case of elastic scattering on a real potential \hat{V}_{aA} , the S matrix elements are complex numbers of unit modulus such that the ingoing and outgoing fluxes in each

partial wave l are identical. In this case the phase shifts δ_l are real quantities that can be limited to the interval $[0, \pi]$ (or $[0^\circ, 180^\circ]$). The asymptotic form of the radial wave functions

$$u_l = \frac{1}{2i} \left[S_l u_l^{(+)} - u_l^{(-)} \right] \quad (66)$$

in equation (61) is then given by

$$u_l(k_i r) \rightarrow \exp(i\delta_l) \sin\left(k_i r + \delta_l - l\frac{\pi}{2}\right). \quad (67)$$

Thus the phase shifts have a simple interpretation, see figure 5. The action of the scattering potential leads to a shift of the phase of the asymptotic radial wave function. The phase shifts δ_l depend on the momentum k_i or the energy E_{aA} in the initial state. In most cases one finds a smooth variation where an increase (decrease) of δ_l usually signifies an attractive (repulsive) potential, see figure 6. A sharp increase of the phase shift from values near 0° through 90° to 180° corresponds to a resonant behavior that can be observed in the cross section. According to equation (52), the differential cross section for elastic scattering ($v_i = v_f$) assumes the form

$$\frac{d\sigma_{ii}}{d\Omega} = \left| \sum_l \frac{2l+1}{2ik_i} [S_l(k_i) - 1] P_l(\cos\theta) \right|^2 \quad (68)$$

including the full angular dependence. An integration over all solid angles gives the total elastic scattering cross section

$$\sigma_{\text{el}} = \int d\Omega \frac{d\sigma_{ii}}{d\Omega} = \frac{\pi}{k_i^2} \sum_l (2l+1) |S_l(k_i) - 1|^2 \quad (69)$$

where the orthogonality of Legendre polynomials

$$\int_{-1}^1 dz P_l(z) P_{l'}(z) = \frac{2}{2l+1} \delta_{ll'} \quad (70)$$

has been used. One easily recognizes that the contribution of a partial wave l to the total elastic cross section is maximal if $S_l = -1$ or $\delta_l = \pi/2$.

If the current J_f in the cross section (52) is calculated from the full scattering wave $\Psi_i^{(+)}$ instead of the scattering part $\Psi_i^{(+)} - \Phi_i$, the absorption cross section

$$\sigma_{\text{abs}} = \frac{\pi}{k_i^2} \sum_l (2l+1) \left[1 - |S_l(k_i)|^2 \right] \quad (71)$$

is obtained after performing the angular integration. For real scattering phase shift δ_l , the modulus of the S matrix elements is one, i.e.,

$$|S_l(k_i)| = |\exp(2i\delta_l)| = 1 \quad (72)$$

and the absorption cross section (71) vanishes. A finite value for σ_{abs} is found for complex phase shifts with positive imaginary part $\text{Im}(\delta_l) > 0$ since then

$$|S_l(k_i)| = \exp[-2\text{Im}(\delta_l)] < 1. \quad (73)$$

A positive absorption cross section is connected to the removal of flux from the elastic scattering channel. This can be realized phenomenologically by introducing an optical potential $U = V + iW$ for V_{aA} with real and imaginary contributions (V, W real) [26, 27]. The total reaction cross section

$$\sigma_{\text{tot}} = \sigma_{\text{el}} + \sigma_{\text{abs}} = \frac{2\pi}{k_i^2} \sum_l (2l+1) \text{Re}[1 - S_l(k_i)] \quad (74)$$

is given by the sum of the elastic and absorption cross sections. It is related to the imaginary part of the forward scattering amplitude, i.e. $f_{ii}^{(+)}(\theta)$ for $\theta = 0$, by the so-called optical theorem

$$\sigma_{\text{tot}} = \frac{4\pi}{k_i} \text{Im} \left[f_{ii}^{(+)}(0) \right] \quad (75)$$

because $P_l(1) = 1$.

The resonant behavior of the elastic phase shift in a partial wave l can be parametrized near a resonance at energy E_r with narrow width $\Gamma \ll E_r$ by an energy dependence of the S matrix element in the form

$$S_l(E) = \frac{E - E_r - i\frac{\Gamma}{2}}{E - E_r + i\frac{\Gamma}{2}}. \quad (76)$$

It is evident that $|S_l(E)| = 1$. Using

$$S_l(E) - 1 = -i \frac{\Gamma}{E - E_r + i\frac{\Gamma}{2}} \quad (77)$$

the contribution of this partial wave to the elastic scattering cross section

$$\sigma_{\text{el}}^{(l)} = \frac{\pi}{k_i^2} (2l+1) \frac{\Gamma^2}{(E - E_r)^2 + \frac{\Gamma^2}{4}} \quad (78)$$

shows the typical Breit-Wigner shape with a maximum at $E = E_r$ with $S_l(E_r) = -1$ and $\delta_l(E_r) = \pi/2$. A general formulation of cross sections with many resonances and many channels including effects of the Coulomb potentials is realized in the so-called R matrix theory [22–24]. The relevant parameters are formal resonance energies and reduced widths.

2.4.2 Operator formalism

An alternative approach to obtain the full scattering wave function relies on a reformulation of the problem as an integral equation. For the simplification of the notation, the internal structure of the scattered particles is not explicitly indicated in the following. Thus one sets $\phi_a = \phi_A = 1$ and $E_a = E_A = 0$. The full Schrödinger equation is written as

$$\hat{H}\Psi^{(\pm)} = \left(\hat{T} + \hat{V} \right) \Psi^{(\pm)} = E\Psi^{(\pm)} \quad (79)$$

with energy $E = E_i = E_{aA} = \hbar^2 k_i^2 / (2\mu_{aA})$. The Hamiltonian without interaction potential \hat{V} reduces to the kinetic contribution of relative motion

$$\hat{H}_0 = \hat{T} = -\frac{\hbar^2}{2\mu_{aA}} \Delta \quad (80)$$

with the plane-wave solution

$$\Phi_0(\mathbf{k}_i) = \exp(i\mathbf{k}_i \cdot \mathbf{r}) \quad (81)$$

for the Schrödinger equation $\hat{H}_0\Phi_0 = E\Phi_0$. The full equation (79) can be rearranged in the form

$$\hat{V}\Psi = (E - \hat{H}_0)\Psi. \quad (82)$$

This motivates to define the operator

$$\mathcal{G}_0^{(\pm)} = (E - \hat{H}_0 \pm i\epsilon)^{-1} \quad (83)$$

to reformulate the problem. The imaginary term with ϵ is introduced in order to circumvent the singularity on the real axis and to incorporate the correct boundary conditions. It is always to be understood that all equations have to be taken in the limit $\epsilon \rightarrow 0$. Then the equivalent to equation (79) is obtained as

$$\Psi^{(\pm)} = \Phi_0(\mathbf{k}_i) + \mathcal{G}_0^{(\pm)}\hat{V}\Psi^{(\pm)}, \quad (84)$$

often called Lippmann-Schwinger equation. More explicitly, this equation reads

$$\begin{aligned} \Psi^{(\pm)}(\mathbf{r}) &= \Phi_0(\mathbf{k}_i, \mathbf{r}) \\ &+ \int d^3r' G_0^{(\pm)}(\mathbf{r}, \mathbf{r}')\hat{V}(\mathbf{r}')\Psi^{(\pm)}(\mathbf{r}') \end{aligned} \quad (85)$$

with the Green's function

$$G_0^{(\pm)}(\mathbf{r}, \mathbf{r}') = -\frac{2\mu_{aA}}{\hbar^2} \frac{\exp(\pm ik_i|\mathbf{r} - \mathbf{r}'|)}{4\pi|\mathbf{r} - \mathbf{r}'|} \quad (86)$$

depending on two arguments \mathbf{r} and \mathbf{r}' . For a vanishing potential \hat{V} the correct solution is immediately found with equation (84). In the general case, however, it is an implicit relation in order to determine $\Psi^{(\pm)}$ since it appears on both sides of the equal sign. By repeated insertions, the explicit formal solution

$$\Psi^{(\pm)} = \Phi_0(\mathbf{k}_i) + \mathcal{G}_0^{(\pm)}\hat{V}\Phi_0 + \mathcal{G}_0^{(\pm)}\hat{V}\mathcal{G}_0^{(\pm)}\hat{V}\Phi_0 + \dots, \quad (87)$$

called Born series, with the integral operator

$$\mathcal{G}_0^{(\pm)}[\dots] = \int d^3r' G_0^{(\pm)}(\mathbf{r}, \mathbf{r}')[\dots] \quad (88)$$

is obtained. Unfortunately, it is difficult to make definite statements about the convergence of this series and hence this solution is not really helpful in actual calculations.

The connection with the scattering amplitude is found by considering the limit of large $r = |\mathbf{r}|$ in the Green's function (86). For $r \gg r'$ (the relevant range of r' is limited by the range of the potential \hat{V}) one has

$$k_i|\mathbf{r} - \mathbf{r}'| \approx k_i r - \mathbf{k}_f \cdot \mathbf{r}' + \dots \quad (89)$$

with $\mathbf{k}_f = k_i\mathbf{r}/r$ and the asymptotic relation

$$\begin{aligned} \Psi^{(\pm)} &\rightarrow \Phi_0(\mathbf{k}_i, \mathbf{r}) - \frac{2\mu_{aA}}{\hbar^2} \frac{\exp(\pm ik_i r)}{4\pi r} \\ &\times \int d^3r' \exp(-i\mathbf{k}_f \cdot \mathbf{r}')\hat{V}(\mathbf{r}')\Psi^{(\pm)}(\mathbf{r}') \end{aligned} \quad (90)$$

is derived. A comparison with equation (46) enables to identify the scattering amplitude

$$f_{fi}^{(\pm)} = -\frac{\mu_{aA}}{2\pi\hbar^2} \int d^3r' \exp(-i\mathbf{k}_f \cdot \mathbf{r}')\hat{V}(\mathbf{r}')\Psi^{(\pm)}(\mathbf{r}') \quad (91)$$

as an integral containing the full wave function, the potential and a plane wave. This relation can also be written as

$$f_{fi}^{(\pm)} = -\frac{\mu_{aA}}{2\pi\hbar^2} T_{fi} \quad (92)$$

with the so-called T matrix element

$$T_{fi} = \langle \Phi_0(\mathbf{k}_f) | \hat{V} | \Psi^{(+)}(\mathbf{k}_i) \rangle. \quad (93)$$

One sees that the knowledge of the T matrix element is sufficient to calculate the cross section, however, the full solution $\Psi^{(+)}$ of the scattering problem is still required.

In some cases it is possible to introduce a potential \hat{U} such that the solution $\chi^{(\pm)}$ of the Schrödinger equation

$$(\hat{H}_0 + \hat{U})\chi^{(\pm)} = E\chi^{(\pm)} \quad (94)$$

is explicitly known. With help of the operator identity

$$\frac{1}{A} - \frac{1}{B} = \frac{1}{B} (B - A) \frac{1}{A} \quad (95)$$

the T matrix element can be split into two contributions

$$\begin{aligned} T_{fi} &= \langle \Phi_0(\mathbf{k}_f) | \hat{U} | \chi^{(+)}(\mathbf{k}_i) \rangle \\ &+ \langle \chi^{(-)}(\mathbf{k}_f) | \hat{V} - \hat{U} | \Psi^{(+)}(\mathbf{k}_i) \rangle. \end{aligned} \quad (96)$$

The potential \hat{U} is often chosen as an optical potential for the relative motion of the scattering particles. The two-potential formula (96) can be generalized to the description of reactions $A(a, b)B$ as

$$\begin{aligned} T_{fi} &= \langle \phi_b \phi_B \Phi_0(\mathbf{k}_f) | \hat{U}_{aA} | \phi_a \phi_A \chi_{aA}^{(+)}(\mathbf{k}_i) \rangle \\ &+ \langle \phi_b \phi_B \chi_{bB}^{(-)}(\mathbf{k}_f) | \hat{V}_{bB} - \hat{U}_{bB} | \Psi_{aA}^{(+)}(\mathbf{k}_i) \rangle \end{aligned} \quad (97)$$

using the Gell-Mann–Goldberger relation [25]. For reactions with $aA \neq bB$ and suitable choice of the potential \hat{U}_{aA} that cannot cause a transition from $A + a$ to $B + b$, one has

$$\langle \phi_b \phi_B \Phi_0(\mathbf{k}_f) | \hat{U}_{aA} | \phi_a \phi_A \chi_{aA}^{(+)}(\mathbf{k}_i) \rangle = 0 \quad (98)$$

and only one contribution to the T matrix element (97) remains. Therefore one arrives at exact expressions for rearrangement reactions in the 'post form'

$$T_{fi} = \langle \phi_b \phi_B \chi_{bB}^{(-)}(\mathbf{k}_f) | \hat{V}_{bB} - \hat{U}_{bB} | \Psi_{aA}^{(+)}(\mathbf{k}_i) \rangle \quad (99)$$

and an equivalent 'prior form'

$$T_{fi} = \langle \Psi_{bB}^{(-)}(\mathbf{k}_f) | \hat{V}_{aA} - \hat{U}_{aA} | \phi_a \phi_A \chi_{aA}^{(+)}(\mathbf{k}_i) \rangle. \quad (100)$$

They are the starting point of many approximations in theoretical models and calculations of specific types of reactions. The potentials \hat{V}_{aA} and \hat{V}_{bB} depend on the coordinates of all nucleons in the nuclei $A+a$ and $B+b$, respectively. They should be chosen consistently with those used

in microscopic descriptions of the nuclei themselves. In actual calculation, however, this is rarely the case. It will be a challenge in future applications to combine structure and reaction calculations selfconsistently with the same microscopic potentials.

Optical potentials that are used in calculations of T matrix elements can be taken from different sources, see, e.g., reference [28]. There are systematic potentials from fits of elastic scattering cross sections for a large range of targets and energies. They are mostly available for the scattering of nucleons and light nuclei, e.g. deuterons and α -particles. However, for exotic nuclei, these systematic potentials are not available. Here, other approaches are more commonly used such as single- or double-folding potentials or potentials derived with the help of dispersive methods. The imaginary part of the optical potential describes the loss of flux to open channels in a particular reaction. It should be treated consistently when open channels are taken explicitly into account in the determination of the scattering wave function.

2.4.3 General cross sections

There is a general formalism to derive expressions for cross sections of arbitrary reactions if the T matrix element is given. It is closely related to Fermi's golden rule that is employed in processes that describe the transition between different states. In the following, spins of the particles are included in the formulas, however only cross sections with unpolarized particles are considered. In a nonrelativistic framework it is useful to work in the center-of-mass (c.m.) system and to introduce relative and c.m. coordinates. In the initial channel of a reaction $A(a, b)B$, one defines the vectors

$$\mathbf{r}_{aA} = \mathbf{r}_a - \mathbf{r}_A, \quad (101)$$

$$\mathbf{R} = \frac{m_a \mathbf{r}_a + m_A \mathbf{r}_A}{m_a + m_A} \quad (102)$$

in coordinate space and conjugate vectors

$$\mathbf{p}_{aA} = \mu_{aA} \left(\frac{\mathbf{p}_a}{m_a} - \frac{\mathbf{p}_A}{m_A} \right), \quad (103)$$

$$\mathbf{P} = \mathbf{p}_a + \mathbf{p}_A \quad (104)$$

in momentum space. Similar expressions can be given for the final state. Then, the energies in the initial and final state (including rest masses) can be written as

$$E_i = E_a + E_A + \frac{p_{aA}^2}{2\mu_{aA}} \quad (105)$$

and

$$E_f = E_b + E_B + \frac{p_{bB}^2}{2\mu_{bB}}, \quad (106)$$

respectively, with relative momenta \mathbf{p}_{aA} and \mathbf{p}_{bB} . The cross section in the c.m. system has the general form

$$d\sigma(a + A \rightarrow b + B) = \quad (107)$$

$$\frac{2\pi}{\hbar} \frac{\mu_{aA}}{p_{aA}} \frac{1}{(2J_a + 1)(2J_A + 1)} \sum_{M_a, M_A} \sum_{M_b, M_B} \times \int \frac{d^3 p_{bB}}{(2\pi\hbar)^3} |T_{(bB)(aA)}|^2 \delta(E_i - E_f + Q_{a+A \rightarrow b+B})$$

where every term has a clear meaning. The factor μ_{aA}/p_{aA} is the inverse of the relative velocity or flux in the initial channel. The summation over the projections M_a and M_A and division by $(2J_a + 1)(2J_A + 1)$ corresponds to an averaging over all possible spin states in the initial channel. The summation over M_b, M_B is performed since there is usually no discrimination of particular spin states in the detection. The integration over all momenta \mathbf{p}_{bB} with corresponding normalization factor $(2\pi\hbar)^3$ covers the full phase space in the final state. Finally, the δ function encodes the conservation of energy. The conservation of the total momentum is guaranteed by the formulation with relative momenta only in equation (107). Using

$$d^3 p_{bB} = p_{bB}^2 dp_{bB} d\Omega_{bB} \quad (108)$$

and

$$\frac{dE_f}{dp_{bB}} = \frac{p_{bB}}{\mu_{bB}} \quad (109)$$

the integration over the modulus of the final state momentum p_{bB} gives the final expression

$$\frac{d\sigma}{d\Omega_{bB}}(a + A \rightarrow b + B) = \frac{\mu_{aA} \mu_{bB}}{(2\pi)^2 \hbar^4} \frac{p_{bB}}{p_{aA}} \times \frac{1}{(2J_a + 1)(2J_A + 1)} \sum_{M_a, M_A} \sum_{M_b, M_B} |T_{(bB)(aA)}|^2 \quad (110)$$

consistent with previous results in sections 2.4.1 and 2.4.2. The cross section for the reaction with two particles in the final state depends on two independent angles corresponding to the direction of the final relative momentum $\hat{p}_{bB} = \mathbf{p}_{bB}/p_{bB}$. The number of six independent kinematical quantities in the final state (three for each particle) reduces to three because of the choice of the c.m. system and further to two due to energy conservation. Hence, $d\sigma/d\Omega_{bB}$ depends on two independent angles. With the dimension $[T_{fi}] = EL^3$, E denoting an energy, the dimension of the cross section becomes $[d\sigma/d\Omega_{bB}] = L^2$ as expected. The case of a reaction with three particles in the final state will be treated below.

The expression for the cross section of the inverse reaction $B(b, a)A$ is easily found as

$$\frac{d\sigma}{d\Omega_{aA}}(b + B \rightarrow a + A) = \frac{\mu_{aA} \mu_{bB}}{(2\pi)^2 \hbar^4} \frac{p_{aA}}{p_{bB}} \times \frac{1}{(2J_b + 1)(2J_B + 1)} \sum_{M_b, M_B} \sum_{M_a, M_A} |T_{(aA)(bB)}|^2 \quad (111)$$

in full analogy to equation (110). Time-reversal symmetry of the two reactions connects the corresponding T matrix elements such that

$$|T_{(bB)(aA)}|^2 = |T_{(aA)(bB)}|^2. \quad (112)$$

A combination of the expressions leads to the theorem of detailed balance

$$(2J_a + 1)(2J_A + 1)p_{aA}^2 \frac{d\sigma}{d\Omega_{bB}}(a + A \rightarrow b + B) \quad (113)$$

$$= (2J_b + 1)(2J_B + 1)p_{bB}^2 \frac{d\sigma}{d\Omega_{aA}}(b + B \rightarrow a + A),$$

which can be used to relate cross section of two mutually inverse reactions. See section 3.1.2 for an application.

The situation is more complex if there are more than two particles in the final state. For a reaction $A(a, Cc)b$ with three ejectiles, there are three possible choices to define relative or so-called Jacobi coordinates. One option is to introduce the relative vector for the system $C + c$ first as

$$\mathbf{r}_{cC} = \mathbf{r}_c - \mathbf{r}_C \quad (114)$$

and then that for the third particle b relative to the $B = C + c$ system with

$$\mathbf{r}_{b(cC)} = \mathbf{r}_{bB} = \mathbf{r}_b - \mathbf{r}_B \quad (115)$$

where

$$\mathbf{r}_B = \frac{m_c \mathbf{r}_c + m_C \mathbf{r}_C}{m_c + m_C} \quad (116)$$

is the c.m. coordinate of the system B . Finally, the c.m. vector of the total system is given by

$$\mathbf{R} = \frac{m_b \mathbf{r}_b + m_c \mathbf{r}_c + m_C \mathbf{r}_C}{m_b + m_c + m_C}. \quad (117)$$

The conjugate momenta are defined as

$$\mathbf{p}_{cC} = \mu_{cC} \left(\frac{\mathbf{p}_c}{m_c} - \frac{\mathbf{p}_C}{m_C} \right), \quad (118)$$

$$\mathbf{p}_{b(cC)} = \mathbf{p}_{bB} = \mu_{bB} \left(\frac{\mathbf{p}_b}{m_b} - \frac{\mathbf{p}_B}{m_B} \right) \quad (119)$$

and

$$\mathbf{P} = \mathbf{p}_b + \mathbf{p}_c + \mathbf{p}_C \quad (120)$$

with

$$\mathbf{p}_B = \mathbf{p}_c + \mathbf{p}_C \quad (121)$$

and the masses $m_B = m_c + m_C$ and $\mu_{bB} = m_b m_B / (m_b + m_B)$. The energy in the final state

$$E_f = E_b + E_c + E_C + \frac{p_{cC}^2}{2\mu_{cC}} + \frac{p_{bB}^2}{2\mu_{bB}} \quad (122)$$

contains two kinetic contributions. Formula (107) for the cross section is easily generalized to

$$d\sigma(a + A \rightarrow b + c + C) = \quad (123)$$

$$\frac{2\pi}{\hbar} \frac{\mu_{aA}}{p_{aA}} \frac{1}{(2J_a + 1)(2J_A + 1)} \sum_{M_a, M_A} \sum_{M_b, M_c, M_C}$$

$$\times \int \frac{d^3 p_{bB}}{(2\pi\hbar)^3} \frac{d^3 p_{cC}}{(2\pi\hbar)^3} |T_{(bcC)(aB)}|^2$$

$$\times \delta(E_i - E_f + Q_{a+A \rightarrow b+c+C})$$

with an additional momentum space integration, the Q value

$$Q_{a+A \rightarrow b+c+C} = (m_a + m_A - m_b + m_c + m_C)c^2, \quad (124)$$

and the T matrix element $T_{(bcC)(aB)}$. With

$$d^3 p_{cC} = p_{cC}^2 dp_{cC} d\Omega_{cC} \quad (125)$$

and

$$\frac{dE_{cC}}{dp_{cC}} = \frac{p_{cC}}{\mu_{cC}} \quad (126)$$

one integration can be performed explicitly and the result

$$\frac{d^3 \sigma}{dE_{cC} d\Omega_{cC} d\Omega_{bB}}(a + A \rightarrow b + c + C) = \quad (127)$$

$$\frac{\mu_{aA} \mu_{bB} \mu_{cC} p_{bB} p_{cC}}{(2\pi)^5 \hbar^7 p_{aA}}$$

$$\times \frac{1}{(2J_a + 1)(2J_A + 1)} \sum_{M_a, M_A} \sum_{M_b, M_c, M_C} |T_{(bcC)(aB)}|^2$$

is obtained. This cross section depends on one energy and two solid angles. The dimension is $[d^3 \sigma / dE_{cC} d\Omega_{cC} d\Omega_{bB}] = L^5 E^{-1}$ because $[T_{(bcC)(aA)}] = EL^6$ for the T matrix element, in which an integration over an additional coordinate appears as compared to $T_{(bB)(aA)}$. The cross section (127) contains valuable information on the correlation between the particles b , c , and C in the final state. With a different choice of Jacobi coordinates, formulas for the cross section depending on another set of variables can be derived. Integration over the energy or angles leads to less highly differential cross sections.

3 Applications

Reaction theory is relevant for a large number of applications in nuclear physics. Here, only a few selected examples will be mentioned. This will give an idea about the variety of cases. On the one hand, cross sections of reactions are of interest themselves. Examples are the prediction of production rates of exotic nuclei that are created in fragmentation reactions or the determination of reaction rates for nucleosynthesis in astrophysical models. On the other hand, reactions serve as a tool to study the structure of nuclei. Gross properties like radii and density distribution can be extracted from the analysis of elastic scattering with electrons, protons, etc. or absorption reactions. More detailed investigations of nuclear structure require the use of particularly chosen reaction processes. Specific states can be populated by the excitation with the electromagnetic or nuclear interaction. Transfer and breakup reactions are chosen in order to study the single-particle structure of nuclei. Reaction studies with exotic nuclei pose particular challenges. Continuum states have to be treated correctly and consistently with bound states. Reaction theory needs to be combined with modern structure models in a novel way. A particular question is the choice of the nuclear interaction that should be based on the most recent advances in that field. In the following, two applications will be discussed in more detail since they exhibit important features of reaction theory.

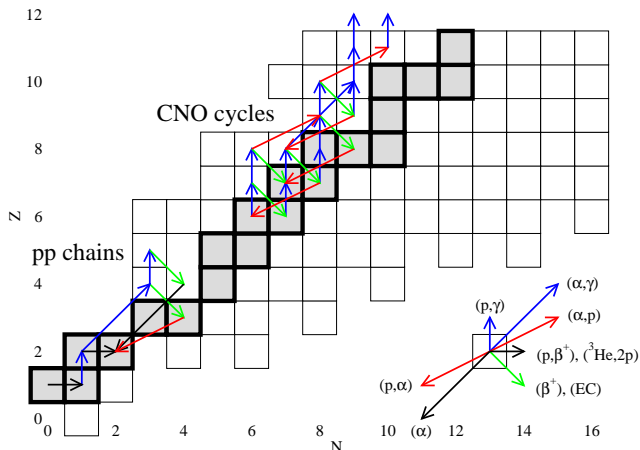


Fig. 7. Reactions in the chart of nuclei that are relevant for the pp chains and CNO cycles of stellar burning. Stable nuclei are indicated by grey squares.

3.1 Indirect methods for nuclear astrophysics

Nuclear reaction rates are an essential input for several astrophysical models, in particular in the study of nucleosynthesis through various processes [29]. Examples are the pp chains and CNO cycles, see figure 7, which are important in stellar burning, or s, r, p, or rp processes, which are connected to the creation of heavy elements. In many cases unstable nuclei are involved and the reaction cross sections are needed at very low energies where a direct measurement in the laboratory is practically impossible. Indirect methods offer an alternative to determine the required cross sections.

In an astrophysical environment, nuclei are immersed in a hot plasma and they acquire a temperature or energy dependent distribution of velocities. The relevant quantity is the Maxwellian-averaged reaction rate

$$r_{aA} = \frac{\rho_a \rho_A}{1 + \delta_{aA}} \langle \sigma v \rangle \quad (128)$$

with the integral

$$\langle \sigma v \rangle = \sqrt{\frac{8}{\pi \mu_{aA}}} \int \frac{dE}{(kT)^{3/2}} E \sigma(E) \exp\left(-\frac{E}{kT}\right) \quad (129)$$

that contains the energy dependent cross section $\sigma(E)$. The Maxwellian energy distribution and the cross section exhibit a very different energy dependence, leading to a well-peaked integrand in equation (129) as depicted in figure 8. For reactions with charged particles, the most effective energy, at which the integrand reaches its maximum, can be estimated to be

$$E_{\text{eff}} = 0.1220 \mu_{aA}^{1/3} (Z_a Z_A T_9)^{2/3} \text{ MeV} \quad (130)$$

with the effective mass μ_{aA} in atomic mass units (amu) and the temperature $T_9 = T/(10^9 \text{K})$. Only energies close to E_{eff} inside the Gamov window are significant in the

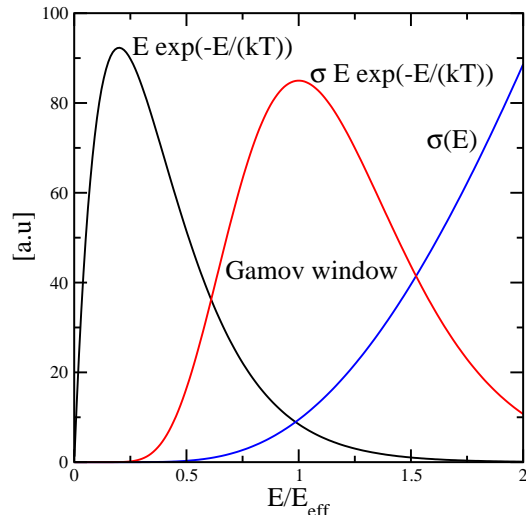


Fig. 8. Energy dependence of the Maxwellian energy distribution (black), cross section (blue) and total integrand (red) in the integral (129).

calculation of the integral. The strong suppression of the cross section $\sigma(E)$ at low energies is a result of the Coulomb repulsion of the colliding nuclei. Effects of the Coulomb potential in scattering can be incorporated rather easily in the theoretical description since the nonrelativistic two-body problem can be solved analytically.

3.1.1 Scattering with Coulomb interaction

Due to the long range of the Coulomb potential

$$V_{\text{Coul}} = \frac{Z_a Z_A e^2}{r} \quad (131)$$

between two nuclei with charge numbers Z_a and Z_A at distance r , the standard description of scattering has to be modified as compared to the formulation that was presented in section 2.4.1. The asymptotic form of the radial wave functions (66) has to be replaced by

$$u_l \rightarrow \frac{\exp(2i\sigma_l)}{2i} [S_l u_l^{(+)} - u_l^{(-)}] \quad (132)$$

with new functions

$$u_l^{(\pm)}(k_i r) = \exp(\mp i\sigma_l) [G_l(k_i r) \pm iF_l(k_i r)] \quad (133)$$

in terms of the regular and irregular Coulomb functions F_l and G_l [21]. Their asymptotic behavior is given by

$$u_l^{(\pm)}(k_i r) \rightarrow \exp\left\{\pm i \left[k_i r - 2\eta \ln(k_i r) + \sigma_l - l\frac{\pi}{2} \right]\right\} \quad (134)$$

with the Coulomb phase shifts

$$\sigma_l = \arg \Gamma(l + 1 + i\eta). \quad (135)$$

They depend on the Sommerfeld parameter

$$\eta = \frac{Z_a Z_A e^2}{\hbar v_{aA}} \quad (136)$$

containing the relative velocity $v_{aA} = p_{aA}/\mu_{aA}$. The partial-wave expansion of the elastic scattering amplitude takes the form

$$f_{ii}^{(+)}(\theta) = \sum_l \frac{2l+1}{2ik_i} [\exp(2i\sigma_l) S_l(k_i) - 1] P_l(\cos\theta) \quad (137)$$

with the appearance of an additional factor in front of the nuclear S-matrix element S_l . It is convenient to split the scattering amplitude into two contributions

$$f_{ii}^{(+)} = f_C^{(+)}(\theta) + f_N^{(+)}(\theta) \quad (138)$$

with the pure Coulomb part

$$\begin{aligned} f_C^{(+)}(\theta) &= \sum_l \frac{2l+1}{2ik_i} [\exp(2i\sigma_l) - 1] P_l(\cos\theta) \quad (139) \\ &= -\frac{\eta}{2k_i \sin^2(\frac{\theta}{2})} \exp\left[-i\eta \ln \sin^2\left(\frac{\theta}{2}\right) + 2i\sigma_0\right] \end{aligned}$$

and the nuclear part

$$\begin{aligned} f_N^{(+)}(\theta) &= \quad (140) \\ &= \sum_l \frac{2l+1}{2ik_i} \exp(2i\sigma_l) [S_l(k_i) - 1] P_l(\cos\theta). \end{aligned}$$

From (139) the Rutherford scattering cross section (26) is immediately obtained. In the case of scattering with Coulomb and nuclear interactions, an interference terms appears in the elastic scattering cross section

$$\frac{d\sigma_{ii}}{d\Omega} = \left| f_C^{(+)} \right|^2 + 2\text{Re} \left(f_C^{(+)} f_N^{(+)*} \right) + \left| f_N^{(+)} \right|^2 \quad (141)$$

that can dramatically change the angular dependence.

The amplitudes of the wave functions (133) at infinity and a finite distance R between the particles are not identical. Their comparison leads to the definition of the penetrability factor

$$\begin{aligned} P_l(R) &= \frac{\lim_{r \rightarrow \infty} \left| u_l^{(\pm)}(\eta; k_i r) \right|^2}{\left| u_l^{(\pm)}(\eta; k_i R) \right|^2} \quad (142) \\ &= \frac{1}{F_l^2(\eta; k_i R) + G_l^2(\eta; k_i R)}, \end{aligned}$$

which is depicted in figure 9 for the example of elastic $p + {}^7\text{Be}$ scattering as a function of R for partial waves $l = 0, 1$ and 2 and six different energies $E = \hbar^2 k_i^2 / (2\mu_{pBe})$. Several important observations can be made. The penetrability factor decreases rapidly with decreasing distance R , decreasing energy E , and increasing orbital angular momentum l . For $l = 0$, finite values are found in the limit $R \rightarrow 0$ with the explicit result

$$\lim_{R \rightarrow 0} P_0(R) = \frac{2\pi\eta}{\exp(2\pi\eta) - 1}, \quad (143)$$

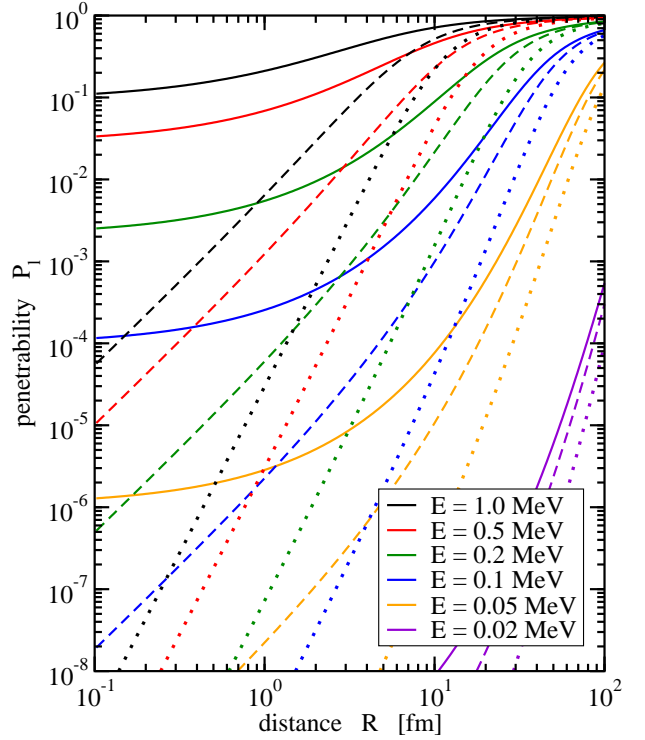


Fig. 9. Penetrability factor $P_l(k_i R)$ in partial waves $l = 0$ (full lines), $l = 1$ (dashed lines), and $l = 2$ (dotted lines) in elastic $p + {}^7\text{Be}$ scattering as a function of the particle distance R for six energies E , decreasing from top to bottom for each set of lines.

which shows a strong decrease with increasing Sommerfeld parameter η . This effect translates into a correspondingly strong energy dependence of the cross sections for reactions with charged particles and explains the extreme difficulties to measure them directly at very low energies in the laboratory. In order to remove the dominating energy dependence due to the Coulomb repulsion, the astrophysical S factor

$$S(E) = \sigma(E) E \exp(2\pi\eta) \quad (144)$$

is introduced in order to obtain a quantity that shows much less variation with energy and can be used for extrapolations of measured data to low energies. However, care has to be taken in this process. Inserting the definition (144) into the integral (129) and assuming a constant value of $S(E)$ leads to the estimate of the most effective energy (130).

3.1.2 Surrogate methods

Because the measurement of low-energy cross sections is so difficult, several methods have been developed to obtain the data in an indirect way. The basic idea is to replace the astrophysically relevant reaction with a closely related surrogate reaction and to make use of reaction theory to extract the required data. The actual realization, of course, depends on the type of reaction that needs to

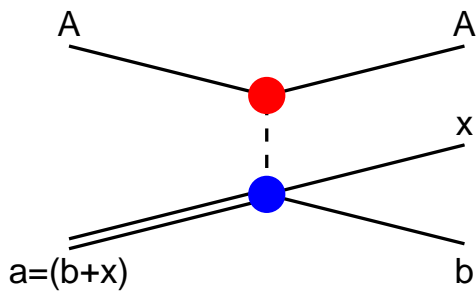


Fig. 10. Diagram of the Coulomb breakup reaction $A(a, bx)A$ with the transfer of a photon (dashed line) between target A and projectile a .

be explored. Here, the following three approaches are considered:

- The Coulomb dissociation (CD) method [18] is used to extract the absolute S factor $S(E)$ as a function of the energy E of a radiative capture reaction $b(x, \gamma)a$ by studying the breakup of particle a in the Coulomb field of a highly-charged target nucleus.
- The asymptotic normalization coefficient (ANC) method [30,31] tries to determine the zero-energy S factor of a radiative capture reaction $b(x, \gamma)a$ from a calculation that uses information on the asymptotic behavior of the bound state wave function of particle a .
- The Trojan-horse (TH) method [32,33] aims at extracting the energy dependence of the S factor for a rearrangement reaction $A(x, c)C$ by using a transfer reaction $A(a, Cc)b$ with three particles in the final state.

In the following, the basic ideas of these methods are discussed in more detail. In general, the three approaches have several common features. A two-body reaction at low energies is replaced by a three-body reaction at 'high' energies. The surrogate reactions can be considered as processes with the transfer of a virtual particle, a photon γ or a nucleus x . Peripheral reactions are studied where the asymptotics of the wave functions is relevant and a selection of suitable kinematic conditions in the experiments is important. Furthermore, approximations are essential in the theoretical description.

The CD method exploits the correspondance of a spectrum of virtual photons with a time-dependent electromagnetic field that a projectile a experiences during the scattering on a highly charged target nucleus A . Thus a breakup reaction $A(a, bx)A$ of a projectile a into fragments b and x is studied experimentally, usually at energies of several hundred MeV per nucleon. The reaction is depicted in diagrammatic form in figure 10 with the transfer of a photon from the target A to the nucleus a . In order to avoid nuclear interactions, large impact parameters or small scattering angles have to be selected. The Coulomb excitation process has been used for a long time to excite stable nuclei in order to study properties of their excited bound states [16,17]. The method is also ideally suited to investigate exotic nuclei since they are usually produced as high-energy beams. Furthermore, their weak binding allows to cross the breakup threshold easily and to access

continuum states. The Coulomb breakup cross section

$$\frac{d^2\sigma}{dE_{bx}d\Omega_{aA}} = \frac{1}{E_\gamma} \sum_{\pi\lambda} \sigma_{\pi\lambda}(a + \gamma \rightarrow b + x) \frac{dn_{\pi\lambda}}{d\Omega_{aA}} \quad (145)$$

can be expressed with the help of photo absorption cross sections $\sigma_{\pi\lambda}(a + \gamma \rightarrow b + x)$. It contains contributions from different electromagnetic multiplicities $\pi = E, M$ and $\lambda = 1, 2, \dots$ with different weights that depend on the virtual or equivalent photon numbers $dn_{\pi\lambda}/d\Omega_{aA}$. The latter depend on the charge number of the target Z_A and the kinematics of the reaction, the scattering angle θ_{aA} or impact parameter b , the projectile velocity v and the excitation (or photon) energy $E_\gamma = \hbar\omega$. They are calculated theoretically in semiclassical approximation, c.f. section 2.3.2, or with quantal methods using scattering wave functions in partial-wave expansion or eikonal approximation. The photon absorption cross sections in equation (145) are finally related to the wanted cross section of the inverse radiative capture reaction via the theorem of detailed balance

$$\sigma_{\pi\lambda}(a + \gamma \rightarrow b + x) = \frac{(2J_b + 1)(2J_B + 1)}{2(2J_a + 1)} \frac{k_{bx}^2}{k_\gamma^2} \sigma_{\pi\lambda}(b + x \rightarrow a + \gamma), \quad (146)$$

cf. equation (113). Since the phase space factor

$$\frac{k_{bx}^2}{k_\gamma^2} = \frac{2\mu_{bx}c^2 E_{bx}}{(E_{bx} + S_{bx})^2} \quad (147)$$

with separation energy S_{bx} for the breakup of a into b and x is very large for not too small relative energies E_{bx} in the $b + x$ system and the virtual photon numbers $dn_{\pi\lambda}/d\Omega_{aA}$ are sizeable for large Z_A and not too high E_{bx} , the Coulomb dissociation cross section is much larger than those of the interesting radiative capture reaction. Hence it is much easier to measure in an experiment. Expression (145) is only valid in the limit of one-photon exchange. Higher-order effects with multi-step transitions or Coulomb post-acceleration in the final state with three charged particles can complicate the application of the method. In order to treat these effects theoretically, better approximations of the full three-body scattering wave function are needed than those employed in the standard approach.

The ANC method and the TH method are applications of transfer reactions. Instead of a photon as in the CD method, a nucleus x is transferred from one nucleus a to another nucleus A . In the final state of the ANC case, see figure 11, particles x and A form a nucleus B in a bound state. In contrast, A and x form a scattering state with two nuclei C and c in the TH approach, see figure 12. Since energy and momentum of particle x are not related by the usual dispersion relation of a free nucleus, it has to be seen as a virtual particle. In the theoretical description of the transfer reaction, which will be detailed in section 3.2, the two vertices in figure 11 contain the information about the breakup of nucleus a into b and x and

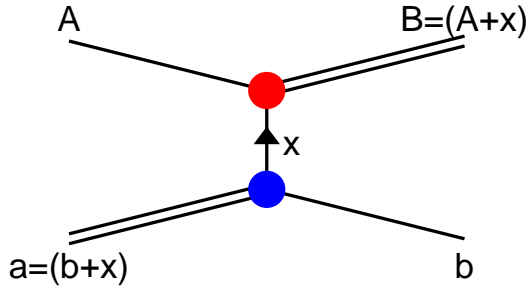


Fig. 11. Diagram of the reaction $A(a, b)B$ for the ANC method with the transfer of a particle x from nucleus a to nucleus A and two particles in the final state.

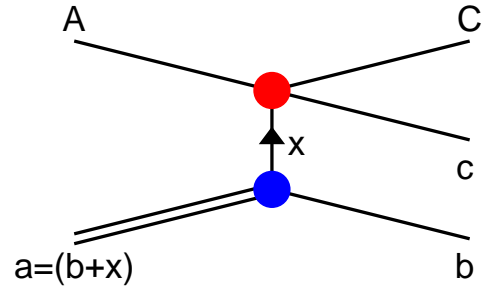


Fig. 12. Diagram of the reaction $A(a, Cc)b$ for the TH method with the transfer of a particle x from nucleus a to nucleus A and three particles in the final state.

the breakup of B into A and x . More precisely, the asymptotic part of the ground state wave function of a (A) enters in the calculation. It determines the cross section of the radiative capture reaction $b(x, \gamma)a$ ($A(x, \gamma)B$) in the limit of zero energy in the state $b+x$ ($A+x$). Since the functional form of the asymptotic wave function is universally given, only its normalization, thus the name of the method, has to be extracted from the measured cross section of the transfer reaction $A(a, b)B$. Since two vertices are involved in the process, one of them has to be known from other experiments. In the TH method, the reaction of interest is the rearrangement reaction $A(x, c)C$ at low energies. A Trojan horse a if formed by attaching a spectator b to the transferred nucleus x . Then the reaction $A(a, Cc)b$ is studied in the laboratory. In the most simple approximations, the cross section for the TH reaction with three particles in the final state can be factorized in three terms. Besides a kinematic factor, there is one factor that is related to the lower vertex in figure 12, describing the breakup of a into b and x , and one factor that corresponds to the upper vertex representing the reaction of interest $A(x, c)C$. Finally, a connection between the cross sections of the reactions $A(a, Cc)b$ and $A(x, c)C$ can be established. An important feature of the TH method is the removal of the Coulomb suppression of the cross section in the former reaction allowing to access very low energies in the latter reaction. For the application, specific kinematical conditions have to be selected such that the momentum transfer to the spectator b is almost negligible. These quasi-free scattering conditions cause particular correlations in the angles of the outgoing particles.

3.2 Transfer reactions

Transfer reactions are a very versatile tool in the application of nuclear reactions. They are used for indirect methods as discussed in the previous section, but are most often applied in the study of nuclear structure. One can distinguish pickup reactions, e.g. (p, d) , (d, t) , $(d, {}^3\text{He})$, or $(d, {}^6\text{Li})$, where the projectile picks up a nucleon or nucleus from the target, and stripping reactions, e.g. (d, p) , (d, n) , or $({}^3\text{He}, p)$, where the projectile deposits a nucleon or nucleus on the target. Apart from these rearrangement

reactions, the theoretical formalism also applies to knock-out and breakup reactions.

The full information on the reaction process is contained in the T matrix elements. An exact calculation of the cross section requires the knowledge of the full scattering wave function $\Psi^{(\pm)}$, see section 2.4.2, which generally is a complicated many-body state. Depending on the type of process, appropriate approximations have to be introduced in order to arrive at manageable calculations. In reactions with stable nuclei, a transfer to bound states with two particles in the final state is often considered. When exotic nuclei are involved, it is frequently the case that three (or more) particles in the final state are emerging and a transfer to continuum states has to be modeled. In the following only the former case $A(a, b)B$ with $Aa \neq Bb$, $a+b+x$ and $B = A+x$ is treated, which corresponds to the process depicted in diagram 11.

3.2.1 Distorted wave Born approximation and spectroscopic factors

The exact T matrix element is given by the post or prior form in equations (99) or (100), respectively. It still contains the exact scattering wave functions $\Psi_{Aa}^{(+)}$ or $\Psi_{Bb}^{(-)}$. In the widely used distorted-wave Born approximation (DWBA), they are replaced by the products

$$\Psi_{Aa}^{(+)} \rightarrow \phi_A \phi_a \chi_{Aa}^{(+)} \quad (148)$$

or

$$\Psi_{Bb}^{(-)} \rightarrow \phi_B \phi_b \chi_{Bb}^{(-)} \quad (149)$$

with distorted waves $\chi_{aA}^{(+)}$ or $\chi_{bB}^{(-)}$ that are generated from optical potentials \hat{U}_{aA} or \hat{U}_{bB} , respectively, see section 2.4.2. Then, for the T matrix elements the approximations

$$T_{(Bb)(Aa)} \approx \langle \phi_b \phi_b \chi_{Bb}^{(-)} | \hat{V}_{Bb} - \hat{U}_{Bb} | \phi_a \phi_a \chi_{Aa}^{(+)} \rangle \quad (150)$$

and

$$T_{(Bb)(Aa)} \approx \langle \phi_b \phi_b \chi_{Bb}^{(-)} | \hat{V}_{Aa} - \hat{U}_{Aa} | \phi_a \phi_a \chi_{Aa}^{(+)} \rangle \quad (151)$$

are found that only differ in the operators but not in the wave functions. It is beneficial to introduce the overlap integrals

$$\Phi_{bx}^a = \langle \phi_b | \phi_a \rangle \quad (152)$$

and

$$\Phi_{Ax}^B = \langle \phi_A | \phi_B \rangle \quad (153)$$

where the integration includes only the coordinates of the nucleons inside b and A , respectively, and the remaining coordinates of the nucleons inside x are left untouched. Hence the overlap integrals can be interpreted as the wave function of the transferred particle. This leads to the expressions

$$T_{(Bb)(Aa)} \approx \langle \Phi_{Ax}^B \chi_{Bb}^{(-)} | \hat{V}_{Bb} - \hat{U}_{Bb} | \Phi_{bx}^a \chi_{aA}^{(+)} \rangle \quad (154)$$

and

$$T_{(Bb)(Aa)} \approx \langle \chi_{bB}^{(-)} \Phi_{Ax}^B | \hat{V}_{Aa} - \hat{U}_{Aa} | \Phi_{bx}^a \chi_{aA}^{(+)} \rangle \quad (155)$$

for the T matrix elements which are still high-dimensional integrals because the functions Φ_{bx}^a and Φ_{Ax}^B depend on the internal coordinates of the transferred particle x and the coordinate of relative motion \mathbf{r}_{bx} and \mathbf{r}_{Ax} , respectively. In principle, they can be obtained from the full many-body wave functions ϕ_b and ϕ_a or ϕ_A and ϕ_B . However, this is rarely the case and it is common practice to approximate them as products

$$\Phi_{bx}^a \approx \mathcal{A}_{bx}^a \varphi_{bx}^a(\mathbf{r}_{bx}) \phi_x \quad (156)$$

and

$$\Phi_{Ax}^B \approx \mathcal{A}_{Ax}^B \varphi_{Ax}^B(\mathbf{r}_{Ax}) \phi_x \quad (157)$$

with spectroscopic amplitudes \mathcal{A}_{bx}^a and \mathcal{A}_{Ax}^B and simple 'single-particle' wave functions $\varphi_{bx}^a(\mathbf{r}_{bx})$ and $\varphi_{Ax}^B(\mathbf{r}_{Ax})$ that are calculated by solving Schrödinger equations for the relative motion with standard potentials, e.g. of Woods-Saxon type. They are normalized to one, i.e.

$$\langle \varphi_{bx}^a | \varphi_{bx}^a \rangle = \langle \varphi_{Ax}^B | \varphi_{Ax}^B \rangle = 1. \quad (158)$$

Because the reaction cross section is proportional to the squared modulus of the T matrix element

$$d\sigma \propto |T_{(Bb)(Aa)}|^2 \quad (159)$$

the cross section can be written as

$$d\sigma(A + a \rightarrow B + b) \approx \mathcal{S}_{bx}^a \mathcal{S}_{Ax}^B d\sigma_{\text{sp}}(A + a \rightarrow B + b) \quad (160)$$

with spectroscopic factors

$$\mathcal{S}_{bx}^a = |\mathcal{A}_{bx}^a|^2 \quad (161)$$

and

$$\mathcal{S}_{Ax}^B = |\mathcal{A}_{Ax}^B|^2 \quad (162)$$

and a single-particle cross section $d\sigma_{\text{sp}}$. The latter is calculated with the single-particle T matrix elements

$$T_{(Bb)(Aa)}^{(\text{sp})} \approx \quad (163)$$

$$\langle \varphi_{Ax}^B(\mathbf{r}_{Ax}) \chi_{Bb}^{(-)} | \hat{V}_{Bb} - \hat{U}_{Bb} | \varphi_{bx}^a(\mathbf{r}_{bx}) \chi_{aA}^{(+)} \rangle$$

or

$$T_{(Bb)(Aa)}^{(\text{sp})} \approx \quad (164)$$

$$\langle \varphi_{Ax}^B(\mathbf{r}_{Ax}) \chi_{Bb}^{(-)} | \hat{V}_{Aa} - \hat{U}_{Aa} | \varphi_{bx}^a(\mathbf{r}_{bx}) \chi_{aA}^{(+)} \rangle.$$

In this approximation, the integration involves only two independent vectors in coordinate space.

A comparison of experimentally measured cross section with calculated single-particle cross sections allows to extract experimental spectroscopic factors. They can be compared to theoretical spectroscopic factors that are derived directly from the overlap functions as

$$\mathcal{S}_{bx}^a = \langle \Phi_{bx}^a | \Phi_{bx}^a \rangle \quad (165)$$

and

$$\mathcal{S}_{Ax}^B = \langle \Phi_{Ax}^B | \Phi_{Ax}^B \rangle \quad (166)$$

using microscopic nuclear structure models. Since the overlap wave functions are obtained from a projection of the full many-body wave functions of the compound nuclei, they are not necessarily normalized to one. The deviation from one is a measure of the correlations inside the many-body wave functions. It has to be emphasized that spectroscopic factors are model depended quantities and not real observables [34]. Thus, a comparison of experimental and theoretical spectroscopic factors has to be carried out with caution. Another concern is related to the choice of the potentials in the T matrix elements. The potentials \hat{V}_{aA} and \hat{V}_{bB} are often not consistent with those used to generate the many-body wave functions ϕ_a , ϕ_A , ϕ_b and ϕ_B . Similarly, questions arise whether the choice of the optical potentials \hat{U}_{aA} and \hat{U}_{bB} is appropriate and how sensitive the matrix elements (163) and (164) are to this choice. Other problems can emerge when the bound state B is replaced by a continuum state $c + C$ as in the TH method. Can spectroscopic factors be defined reasonably, e.g., for resonances, and is the representation of the three-body scattering wave function in the product form (153) with a two-body scattering wave function $\phi_B = \Psi_{Cc}^{(-)}$ sufficient?

3.2.2 Coupled-channel approach

In reactions with weakly-bound nuclei the usual DWBA approach is often not satisfactory. Channels beyond those in the initial and final state, in particular if they are open to decay, have to be included explicitly in the determination of the full many-body scattering wave function. Hence the full scattering wave function is represented as a sum

$$\Psi_{aA}^{(+)} = \sum_c \psi_c \quad (167)$$

with contributions from different channels c in addition to i and f . These have the appropriate asymptotic behavior

$$\psi_c \rightarrow \phi_c f_{c(aA)}^{(+)} \frac{\exp(ik_c r_c)}{r_c} \quad (168)$$

with function ϕ_c that describe the internal structure of the nuclei in the relevant partition, i.e. $\phi_c = \phi_a \phi_A$, $\phi_b \phi_B$, etc. The total Hamiltonian can be likewise partitioned

$$\hat{H} = \hat{H}_c + \hat{T}_c + \hat{V}_c \quad (169)$$

according to the channels, e.g., $\hat{H}_c = \hat{H}_a + \hat{H}_A$, $\hat{T}_c = \hat{T}_{Aa}$, $\hat{V}_c = \hat{V}_{aA}$ in the channel $c = a + A$. The stationary Schrödinger equation $\hat{H}\Psi_{aA}^{(+)} = E\Psi_{aA}^{(+)}$ changes into a set of coupled differential equations

$$\langle \phi_c | \hat{T}_c + \hat{V}_c + E_c - E | \psi_c \rangle = - \sum_{c' \neq c} \langle \phi_c | \hat{H} - E | \psi_{c'} \rangle \quad (170)$$

with, e.g., $E_c = E_a + E_A$, $c = a + A$, in the diagonal part, if it is projected onto the individual channels. One problem of this approach is the infinitely large number of channels (different partitions, excited states and partial waves). Hence, a truncation to the most relevant channels is needed. In channels with three or more unbound nuclei, the asymptotic solution of the problem is most often not known and different approximations have to be introduced. Sometimes it is possible to utilize hyperspherical coordinates or suitable product wave functions. For continuum states, there is a continuous spectrum of energies E and the wave functions are not normalizable. A possible way out is the discretization of the continuum by introducing energy bins. For instance, normalizable wave functions

$$\phi_{bcC} = \phi_b \int_{E_{\min}}^{E_{\max}} dE w(E) \Psi_{cC}^{(+)}(E) \quad (171)$$

are constructed with adequate weight functions $w(E)$. This rather complex approach as been implemented with success in the continuum-discretized coupled-channel (CDCC) method [35]. Both single-particle and collective states can be considered in the structural part of the wave functions. The binning of the continuum can be adapted to resonances and the numerical convergence can be tested. In general, this approach is computationally expensive and can hardly be implemented for high-energy reactions but many successful applications of the method have demonstrated the usefulness of the approach.

4 Summary

In this contribution basic concepts of nonrelativistic reaction theory were delineated. At first the notation, the variety of nuclear reactions, typical scales of the problem and conservation laws were presented. Cross sections were introduced as fundamental observables, which can be calculated theoretically in various approaches using classical, semiclassical or fully quantal methods. Stationary scattering theory was discussed in detail in the framework of partial wave expansions and an integral operator formalism. The basic quantities, such as scattering amplitudes, S and T matrices, were defined and the connection to cross sections for reactions with two or three particles in the final state was established.

Indirect methods for nuclear astrophysics and transfer reactions were discussed as typical examples for the application of reaction theory. Three prominent surrogate approaches, the Coulomb dissociation method, the ANC

method and the Trojan horse method, were outlined after examining the effect of the Coulomb interaction in reactions with charged particles. The distorted wave Born approximation, the notion of spectroscopic factors and the description of reactions with coupled-channel methods were covered in connection with the description of rearrangement reactions.

Despite the long history of reaction theory with many seminal developments and successful applications in the analysis of experimental data, there is still the need for a further refinement and evolution of the methods, in particular for the specific conditions of experiments with unstable nuclei. Main challenges are the consistent description of nuclear structure and reactions in unified and more microscopic models, the choice of appropriate and well founded nuclear interactions, as well as the treatment of continuum states, particularly in many-body systems with Coulomb interaction. The availability of extensive computational capabilities will allow to implement also more complex theoretical approaches. A wealth of new and exciting results from radioactive ion beam facilities will challenge the theoretical understanding. This will require to develop novel methods in reaction theory with bright prospects for the future.

References

1. N. Austern, *Direct Nuclear Reaction Theory* (Wiley, New York 1970).
2. C. A. Bertulani and P. Danielewicz, *Introduction to Nuclear Reactions* (CRC Press, Boca Raton FL 2004)
3. Luiz Felipe Canto and Mahir S. Hussein, *Scattering Theory of Molecules, Atoms and Nuclei* (World Scientific Publishing, Singapore 2013)
4. Harald Friedrich, *Scattering Theory*, Lecture Notes in Physics 872 (Springer-Verlag, Berlin 2013)
5. P. Fröbrich and R. Lipperheide, *Theory of Nuclear Reactions* (Clarendon Press, Oxford 1996)
6. Norman K. Glendenning, *Direct Nuclear Reactions* (World Scientific Publishing, Singapore 2004)
7. Marvin L. Goldberger and Kenneth M. Watson, *Collision Theory* (Dover Publications, Mineola N.Y. 2004)
8. Charles J. Joachain, *Quantum Collision Theory* (North Holland, Amsterdam 1983)
9. Roger G. Newton, *Scattering Theory of Waves and Particles* (Springer-Verlag, New York 1982)
10. Hans Paetz gen. Schiek, *Nuclear Reactions Lecture Notes in Physics 882* (Springer-Verlag, Berlin 2014)
11. G. R. Satchler, *Introduction to Nuclear Reactions* (Oxford University Press, Oxford 1990)
12. Alexei G. Sitenko, *Scattering Theory* (Springer-Verlag, Berlin 1991)
13. John R. Taylor, *Scattering Theory: The Quantum Theory of Nonrelativistic Collisions* (Dover Publications, Mineola N.Y. 1983)
14. Ian J. Thompson and Filomena M. Nunes, *Nuclear Reactions for Astrophysics* (Cambridge University Press, Cambridge 2009)
15. Ta-You Wu and Takashi Omura, *Quantum Theory of Scattering* (Dover Publications, Mineola N.Y. 2011)

16. K. Alder, A. Bohr, T. Huus, B. Mottelson and A. Winther, *Rev. Mod. Phys.* **28** (1956) 432.
17. A. Winther and K. Alder, *Nucl. Phys. A* **319** (1979) 518.
18. G. Baur, C. A. Bertulani and H. Rebel, *Nucl. Phys. A* **458** (1986) 188.
19. C. A. Bertulani and G. Baur, *Phys. Rept.* **163** (1988) 299.
20. J. M. Blatt and L. C. Biedenharn, *Rev. Mod. Phys.* **24** (1952) 258.
21. M. Abramowitz and I. A. Stegun (Eds.), *Handbook of Mathematical Functions with Formulas, Graphs, and Mathematical Tables* (Dover Publications, New York 1970)
22. A. M. Lane and R. G. Thomas, *Rev. Mod. Phys.* **30** (1958) 257.
23. C. R. Brune, *Phys. Rev. C* **66** (2002) 044611.
24. R. E. Azuma *et al.*, *Phys. Rev. C* **81** (2010) 045805.
25. M. Gell-Mann and M. L. Goldberger, *Phys. Rev.* **91** (1953) 398.
26. P. E. Hodgson, *Ann. Rev. Nucl. Part. Sci.* **17** (1967) 1.
27. P. E. Hodgson, *The Nucleon Optical Model* (World Scientific Publishing, Singapore 1994)
28. R. Capote *et al.*, *Nuclear Data Sheets* **100** (2009) 3107.
29. Claus E. Rolfs and William S. Rodney, *Cauldrons in the Cosmos* (University of Chicago Press, Chicago IL 1988)
30. H. M. Xu, C. A. Gagliardi, R. E. Tribble, A. M. Mukhamedzhanov and N. K. Timofeyuk, *Phys. Rev. Lett.* **73** (1994) 2027.
31. A. M. Mukhamedzhanov and R. E. Tribble, *Phys. Rev. C* **59** (1999) 3418.
32. G. Baur, *Phys. Lett.* **78B** (1986) 35.
33. C. Spitaleri *et al.*, *Phys. Rev. C* **63** (2001) 055801.
34. T. Duguet, H. Hergert, J. D. Holt and V. Somà, *Phys. Rev. C* **92** (2015) 3, 034313.
35. M. Yahiro, K. Ogata, T. Matsumoto and K. Minomo, *PTEP* **2012** (2012) 01A206.